

Patronus: INTERPRETABLE DIFFUSION MODELS WITH PROTOTYPES

Nina Weng, Aasa Feragen, Siavash Bigdeli

Technical University of Denmark

{ninwe, afhar, sarbi}@dtu.dk

ABSTRACT

Uncovering the opacity of diffusion-based generative models is urgently needed, as their applications continue to expand while their underlying procedures largely remain a black box. With a critical question – how can the diffusion generation process be interpreted and understood? – we proposed *Patronus*, an interpretable diffusion model that incorporates a prototypical network to encode semantics in visual patches, revealing *what* visual patterns are modeled and *where* and *when* they emerge throughout denoising. This interpretability of *Patronus* provides deeper insights into the generative mechanism, enabling the detection of shortcut learning via unwanted correlations and the tracing of semantic emergence across timesteps. We evaluate *Patronus* on four natural image datasets and one medical imaging dataset, demonstrating both faithful interpretability and strong generative performance. With this work, we open new avenues for understanding and steering diffusion models through prototype-based interpretability.

Our code is available at <https://github.com/nina-weng/patronus>.

1 INTRODUCTION

The generative capabilities of modern machine learning models, particularly diffusion models, have advanced significantly, enabling the creation of highly realistic samples that closely resemble real-world data. However, their opacity raises critical concerns, including bias amplification (Luccioni et al., 2023), unsafe content (Qu et al., 2023), and copyright violations (Vyas et al., 2023). Their lack of transparency makes it difficult to detect and mitigate these risks, highlighting a fundamental question: *How can the diffusion generation process be interpreted and understood?* Specifically, **what** visual patterns emerge during generation, **where** and **when** they appear, and to what extent they can be **controlled**. Addressing these questions is essential, not only for improving generative ability but also for ensuring interpretability, transparency, and ethical deployment, aligning with regulatory frameworks such as the EU AI Act.

Existing approaches to improving interpretability in diffusion-based visual generation typically fall into two categories. The first relies on post-hoc analysis to investigate how semantic information are encoded in intermediate representations (Kwon et al., 2022; Lee et al., 2023; Park et al., 2023; Haas et al., 2024). However, this method is inherently retrospective and limited in its ability to provide direct control over generation. The second approach introduces additional encoder-based semantic vectors for diffusion guidance (Preechakul et al., 2022; Leng et al., 2023; Wang et al., 2023b), which improves controllability, but often resulting in representations that are difficult to interpret. Moreover, these methods tend to capture global (e.g. face shape, pose) rather than fine-grained patterns (e.g. hair/make-up details, facial expressions), and the latter are crucial for interpretability.

To address these limitations, we aim to develop a method that fulfills two key objectives: (1) embedding interpretability directly into the model architecture, thereby providing **intrinsic transparency** and eliminating the need for post-hoc analysis of high-dimensional latent features; (2) moving interpretability a step further from global to **local semantic meanings** and enabling the controllability.

In this work, we propose *Patronus*, an interpretable diffusion-based generative model integrated with a prototypical network for semantic encoding (Fig. 1). Our approach trains prototype features to capture localized patterns within image patches, and uses prototype activation vector to encode the presence of semantic information for diffusion guidance. This design effectively reduces the

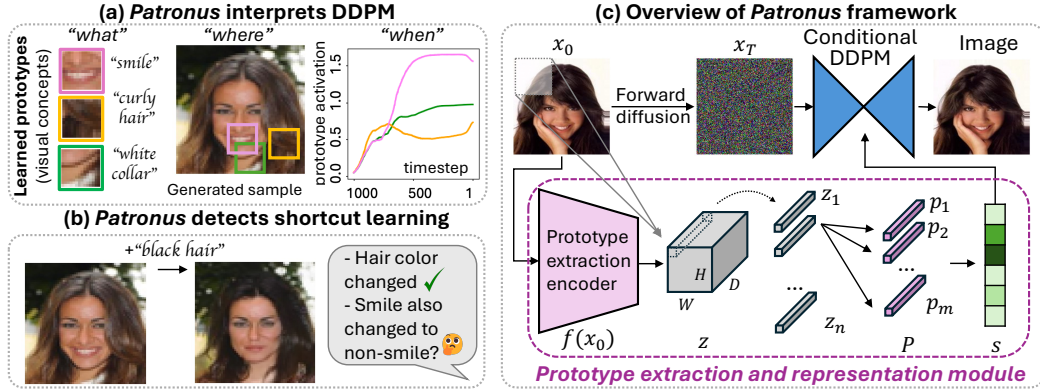


Figure 1: **Proposed *Patronus* model.** (a) **Interpretability**: By integrating a prototypical network as the encoder, *Patronus* learns semantic prototypes (“what”) and explains the generative process by revealing *where* and *when* they emerge. (b) **Diagnosis**: *Patronus* could detect unwanted correlation (e.g., in this case hair color and smile) learned from training data. (c) **Overview of *Patronus***: contains a prototypical network for prototype extraction and a conditional DDPM for generation.

latent dimensionality while preserving sufficient semantic information. *Patronus* allows directly visualizing the semantics of the learned prototypes by manipulating the condition signals on specific prototypes, thereby enhancing interpretability and enabling the diagnosis of shortcut learning. Beyond that, *Patronus* further reveals when prototypes emerge during the denoising process, providing temporal insights and guiding more efficient editing.

Our contributions are summarized as follows:

- We propose *Patronus*: An interpretable diffusion model for image generation which incorporates a prototypical network for prototype learning and representation, alongside a conditional guidance by a prototype activation vector – entirely without extra annotations.
- We introduce a novel method for visualizing learned prototypes, revealing the semantic meanings of them and how they engaged in the generation process.
- Through extensive experiments, we show that *Patronus* effectively captures semantically meaningful features within images, and achieves competitive latent quality and generation quality compared to SOTA methods.
- We empirically demonstrate the potential of *Patronus* to diagnose hidden bias by detecting shortcut learning, offering a valuable tool for mitigating biases in generative models and promoting fairness in their deployment.

2 RELATED WORK

2.1 PROTOTYPE-BASED INTERPRETABILITY

Our work is closely related to and motivated by ProtoPNet (Chen et al., 2019), which builds interpretable deep learning frameworks by learning *prototypes*, intermediate representations of visually similar patterns between training and inference images.

Under such a design, a key challenge is visualizing the learned prototypes. Li et al. (2018) used a decoder to reconstruct prototypes, which resulted in blurry visualizations due to data ambiguity. ProtoPNet instead identified the closest matching encoded representations from the training set via distance comparisons. However, this approach cannot guarantee capturing the true representative mode of the distribution. Follow-up works (Donnelly et al., 2022; Wang et al., 2023a; Ming et al., 2019; Ghosal & Abbasi-Asl, 2021) explore alternative prototype design but *do not* enhance visualization. We propose a new method for prototype visualization that allow finding the most probable visual representation of a prototype. Additionally, the aforementioned studies only focus on *classification*, our work focus on learning and visualizing prototypes for *generative* models.

2.2 INTERPRETABLE DIFFUSION MODELS

Recent work on explaining diffusion models has focused on the following two directions.

Semantic Interpretation of Internal Features. Diffusion models were traditionally viewed as lacking internal representations compared to other generative models, like VAE (Kingma & Welling, 2013) and GAN (Goodfellow et al., 2014). However, Kwon et al. (2022) pointed out that *diffusion models possess a semantic latent space* within the U-Net’s intermediate layer. They leverage the bottleneck for semantic control over the denoising process and propose the asymmetric reverse process to edit the image based on the discovered semantic meaning.

Building on this idea, researchers have sought to interpret the latent space of diffusion models by grouping the latent vectors with different noise schedules (Lee et al., 2023), applying pullback metrics to obtain meaningful local latent basis (Park et al., 2023), and uncovering semantically meaningful directions by both PCA and linear properties of the semantic latent space (Haas et al., 2024). Other works (Si et al., 2024; Tumanyan et al., 2023) extract structural information from the latent space and use it for I2I translation or prompted generation tasks.

This line of work focuses on post-hoc analyses of existing diffusion models, whereas our approach provides *intrinsic* interpretability by design. Moreover, while prior studies often rely on annotated data or external classifiers to uncover the semantic latent space, *Patronus* learns prototypes in a fully *unsupervised* manner.

Autoencoder-based semantic feature extraction for guidance. An alternative way to enhance the interpretability of diffusion models is to integrate an additional encoder to extract semantic features for guidance. DiffAE (Preechakul et al., 2022) pioneered this idea using a learnable encoder for latent semantics. Expanding on this, DiffuseGAE (Leng et al., 2023) proposed a group-supervised AutoEncoder to achieve better latent disentanglement, while InfoDiffusion (Wang et al., 2023b) reduced latent dimensionality and enforced mutual information constraints for more effective learning.

While these methods extract global semantic features, *Patronus* instead captures local features through a prototypical network. Another key distinction lies in how the diffusion model is guided: Rather than direct semantic information, we use the *prototype activation vector*. This approach significantly reduces the dimensionality needed for diffusion guidance while preserving enough capacity in prototype features to encode the same semantic information.

3 PATRONUS: INTERPRETABLE DIFFUSION MODEL

Our proposed model, **Patronus: Prototype-Assisted Transparent Diffusion Model**, is illustrated in Fig. 1c. Designed to enhance transparency and interpretability in diffusion models, *Patronus* incorporates a prototype extraction and representation module (Fig. 1c-bottom). This module learns patch-based prototypes within the image and computes similarity score for each prototype, which are then used to condition the diffusion process (Fig. 1c-top). We elaborate on the details of the prototype extraction and representation module in Sec. 3.1 and the conditional DDPM in Sec. 3.2. Furthermore, we explain how transparency and interpretability are achieved, including sampling strategy and manipulations, in Sec. 3.3. We detail the unconditional sampling strategies in Sec. 3.4, and furthermore prove that adding conditions does not degrade the denoiser training in Sec. 3.5.

3.1 PROTOTYPE EXTRACTION AND REPRESENTATION

This module, inspired by ProtoPNet, consists of two key components: The **prototype encoder** transforms input images into patch-based feature representations. Utilizing the properties of convolutional neural networks (CNNs), each output neuron in the feature map corresponds to a specific patch of the input image, determined by the network’s receptive field. This patch-based representation enables the model to focus on localized patterns and learn fine-grained prototypes. The **activation vector** is derived by calculating similarity scores for each learned prototype, based on the distance between encoded patches and prototypes, where higher scores indicate stronger matches.

This module works as follows: As shown in Fig. 1c, given an input image x_0 , the prototype encoder f extracts features $z = f(x_0)$ into a tensor of shape $H \times W \times D$. In this work, the encoder is a

4-layer Conv-ReLU encoder. The network learns m prototypes in the latent feature space during training, denoted as $P = \{p_j\}_{j=1}^m$, each with the shape $1 \times 1 \times D^1$. Each prototype p_j can be interpreted as a latent encoding of a patch in the original pixel space. This patch, importantly, need not exist in the dataset but should lie within the plausible data distribution.

For the encoder output $z = f(x_0)$, each spatial region within z that corresponds to the same size as a prototype ($1 \times 1 \times D$) can be interpreted as representing a patch of x_0 . Thus, z can be decomposed into smaller regions as follows: $z = \{z_i\}_{i=0}^n$, where n denotes the total number of patches encoded in z . In our case, $n = H \times W$.

To calculate the similarity between the encoded features z and the learned prototypes P , we begin by computing the squared $L2$ distance between each spatial feature z_i and each prototype p_j : $d^2(z_i, p_j) = \|z_i - p_j\|^2$. Next, the minimum distance across the spatial dimensions is selected for each prototype: $d_{min,j}^2 = \max(-d_j^2)$, kernel size = (H, W) , where d_j^2 is the set of distances for the j^{th} prototype across all spatial positions, and the kernel size aligns with the feature map's spatial dimensions H and W . The sequence of minimum distances for all prototypes is converted into an activation vector s using a log transformation: $s = \log(\frac{d^2+1}{d^2+\epsilon})$, where ϵ is a small positive constant.

3.2 CONDITIONAL DIFFUSION PROCESS

Denoising diffusion probabilistic models (DDPM) form a class of generative models that learn data distributions by iteratively denoising a noisy latent representation. The process involves **(1) a forward diffusion process**, where Gaussian noise is progressively added to a data sample x_0 over T timesteps, producing noisy latents x_t , defined as

$$q(x_t | x_{t-1}) = \mathcal{N}(x_t; \sqrt{\alpha_t}x_{t-1}, (1 - \alpha_t)\mathbf{I}). \quad (1)$$

Here, the marginal distribution of x_t given x_0 is:

$$q(x_t | x_0) = \mathcal{N}(x_t; \sqrt{\bar{\alpha}_t}x_0, (1 - \bar{\alpha}_t)\mathbf{I}), \quad (2)$$

where $\bar{\alpha}_t = \prod_{i=1}^t \alpha_i$ and $\alpha_t = 1 - \beta_t$, where β_t is the variance of the Gaussian noise added at t . Furthermore, DDPMs rely on **(2) a reverse generative process** that removes noise given t :

$$p_\theta(x_{t-1} | x_t) = \mathcal{N}(x_{t-1}; \mu_\theta(x_t, t), \Sigma_\theta(x_t, t)). \quad (3)$$

To enable **conditional generation**, we modify the reverse process to be conditioned on the prototype activation vector s . Therefore the updated reverse process is:

$$p_\theta(x_{t-1} | x_t, s) = \mathcal{N}(x_{t-1}; \mu_\theta(x_t, t, s), \Sigma_\theta(x_t, t)). \quad (4)$$

The training objective remains based on the standard noise-prediction loss used in DDPM. For a given noisy sample x_t , timestep t and noise ϵ the model minimizes the loss:

$$\mathcal{L}_{ddpm} = \mathbb{E}_{x_0, \theta, t} [\|\epsilon - \epsilon_\theta(x_t, t, s)\|^2], \quad (5)$$

where ϵ_θ is the learned denoiser. As the loss indicates, our guidance does not change the model's output – it only encourages its reasoning to utilize prototypes for transparency.

3.3 TRANSPARENCY AND INTERPRETABILITY OF PATRONUS

The similarity score s_j quantifies the activation of the j^{th} prototype in a given input, indicating the presence of specific semantic patterns. The model thus conditionally generates samples guided by interpretable semantic information.

Visualizing learned prototypes. Integrating a prototypical network as a semantic meaning extraction module brings inherent interpretability: Each learned prototype vector p_j represents a patch in the image domain. In ProtoPNet, those patches are retrieved by greedily searching all candidate patches in the training set for the closest embeddings.

We argue that the learned prototypes do not need to correspond directly to specific training patches but should instead align with the overall distribution of the training data. To support this, we propose a novel prototype visualization method with the following steps:

¹whose generalization to $H_1 \times W_1 \times D$ as in Chen et al. (2019) is straightforward.

1. Compute the activation vector $s = \{s_j\}_{j=1}^m$, for a given sample x_0 , where s_j represents the similarity score between x_0 and the j_{th} prototype.
2. For target prototype J , increase its similarity score s_J to the plausible maximum while keeping all other scores unchanged. The updated activation vector $s' = \{s'_j\}_{j=1}^m$ is defined as: $s'_j = \begin{cases} s_j, & \text{if } j \neq J \\ \max(s_X), & \text{if } j = J \end{cases}$. Here, s_X represents similarity scores from a representative subset, constraining s_J within a plausible range.
3. Using the updated activation vector s' to sample a new image x' conditioned on s' .
4. Identify the most activated patch x'_i in x' that corresponds to the target prototype J . This patch x'_i serves as the visual representation of p_J .

This method could also be used to visualize prototypes in other prototypical deep learning models.

Manipulation using the prototype activation vector. Manipulating images is a natural downstream task for *Patronus*, as adjusting a specific prototype similarity score s_j and conditionally generating a new sample allows us to effectively and semantically control the image content:

$$p_\theta(x_{t-1} | x_t, s') = \mathcal{N}(x_{t-1}; \mu_\theta(x_t, t, s'), \Sigma_\theta(x_t, t)) \quad (6)$$

Deterministic reverse process via DDIM sampling. Both the visualization of prototypes and their manipulation via activation vectors build on the DDPM sampling process. However, for stricter control over the stochasticity introduced by random noise, the Denoising Diffusion Implicit Models (DDIM) sampler provides an alternative approach. Here, the denoiser is given by $p_\theta(x_{t-1} | x_t, s) = \mathcal{N}(x_{t-1}; \mu_t, \sigma^2 \mathbf{I})$, with mean $\mu_t = \sqrt{\bar{\alpha}_{t-1}} \cdot \hat{x}_0 + \sqrt{1 - \bar{\alpha}_{t-1} - \sigma^2} \cdot \epsilon_\theta(x_t, t, s)$ and variance $\sigma^2 = \eta^2 \cdot \frac{1 - \bar{\alpha}_{t-1}}{1 - \bar{\alpha}_t} \cdot (1 - \frac{\bar{\alpha}_t}{\bar{\alpha}_{t-1}})$. By setting $\eta = 0.0$, the process becomes deterministic, leading to the following update for the reverse process: $x_{t-1} = \sqrt{\bar{\alpha}_{t-1}} \cdot \hat{x}_0 + \sqrt{1 - \bar{\alpha}_{t-1}} \cdot \epsilon_\theta(x_t, t, s)$. Here, \hat{x}_0 is the estimated denoised image, computed as $\hat{x}_0 = \frac{1}{\sqrt{\bar{\alpha}_t}} (x_t - \sqrt{1 - \bar{\alpha}_t} \cdot \epsilon_\theta(x_t, t, s))$.

This DDIM sampling requires x_T , which represents the initial noise in the diffusion process. This could be obtained by performing a deterministic backward generative process, given by $x_{t+1} = \sqrt{\bar{\alpha}_{t+1}} \cdot \hat{x}_0 + \sqrt{1 - \bar{\alpha}_{t+1}} \cdot \epsilon_\theta(x_t, t, s)$.

3.4 UNCONDITIONAL SAMPLING STRATEGY

For unconditional sampling, we train an auxiliary latent diffusion model $p(s_{t-1}|s_t, t)$ to sample s . During training, we first jointly optimize the prototypical encoder with the conditional DDPM; subsequently, the latent diffusion model is trained with the parameters of prototype encoder frozen.

3.5 ADDING THE CONDITION TO THE OBJECTIVE

In *Patronus*, the prototype encoder is jointly optimized with the denoiser. To show that this simultaneous training does not degrade the generated distribution, we analyze how updating the condition s affects the likelihood. For ease of derivation, we use the Evidence Lower Bound (ELBO) as an equivalent objective to generalize denoising losses (Ho et al., 2020).

Proposition. *Any ELBO-improving update for the encoder always leads to progress. Such an update either increases the conditional likelihood of the data under the model or reduces the KL divergence between the generated distribution and the underlying data distribution.*

Proof. Let $z = x_{1:T}$ denote the forward noised latents generated from a fixed forward process $q(z | x)$, as is standard in diffusion models. For parameters s , define the per-sample evidence lower bound (ELBO)

$$\text{ELBO}(x; s) = \mathbb{E}_{q(z|x)} [\log p_\theta(x, z | s) - \log q(z | x)],$$

and the conditional log-likelihood

$$\log p_\theta(x | s) = \text{ELBO}(x; s) + \text{KL}(q(z | x) \| p_\theta(z | x, s)).$$

Consider an update $s^i \mapsto s^{i+1}$ that satisfies $\text{ELBO}(x; s^{i+1}) \geq \text{ELBO}(x; s^i)$ for the data point x . Then the following identity holds:

$$\log p_\theta(x | s^{i+1}) - \log p_\theta(x | s^i) = [\text{ELBO}(x; s^{i+1}) - \text{ELBO}(x; s^i)] + \Delta\text{KL}(x), \quad (7)$$

$$\text{where } \Delta\text{KL}(x) = \text{KL}(q(z | x) \| p_\theta(z | x, s^{i+1})) - \text{KL}(q(z | x) \| p_\theta(z | x, s^i)).$$

Given that the ELBO difference term is positive, Equation 7 implies that one of the following (improving) outcomes must occur:

Conditional likelihood improves. If $\Delta\text{KL}(x) \leq 0$, then

$$\text{KL}(q(z | x) \| p_\theta(z | x, s^{i+1})) \leq \text{KL}(q(z | x) \| p_\theta(z | x, s^i)).$$

meaning that the model posterior $p_\theta(z | x, s^{i+1})$ more closely matches the forward distribution $q(z | x)$. This reduces the gap between the ELBO and the true conditional log-likelihood, yielding a tighter variational bound.

Generated samples become more probable. If $\Delta\text{KL}(x) > 0$ and considering that ELBO is also increased, then necessarily

$$\log p_\theta(x | s^{i+1}) \geq \log p_\theta(x | s^i),$$

i.e. the model assigns higher probability to x .

Hence, any update of the encoder that increases the ELBO either increases the conditional likelihood of the data or reduces the KL divergence between the model posterior and the forward process, guaranteeing progress in approximating the data distribution. \square

This analysis is inapplicable under alternative training objectives for latent condition (e.g., InfoDiff).

4 EXPERIMENTS AND RESULTS

In our experiments, we first assess the semantic meaning of learned prototypes (Sec. 4.1) through reconstruction, interpolation, extrapolation, and manipulation tasks. We also investigate prototype visualization and their consistency. We then analyze prototype quality and generation performance (Sec. 4.2, 4.3). Finally, we explore how *Patronus* aids in diagnosing shortcut learning in diffusion models by identifying potentially unwanted correlations via prototype similarity scores (Sec. 4.4).

We use five datasets: Quantitative evaluation on FMNIST (Xiao et al., 2017), CIFAR-10 (Krizhevsky et al., 2009), FFHQ (Karras, 2019); qualitative analysis on CheXpert (Irvin et al., 2019); and in-depth quantitative and qualitative experiments on CelebA (Liu et al., 2015). We use 100 prototypes for all datasets except FMNIST, which has 30. Prototypes are encoded with a shape of (1,1,128).

4.1 SEMANTIC MEANING OF THE LEARNED PROTOTYPES.

We firstly verify that the learned prototypes are *semantically meaningful* by the following analyses.

Reconstructing image semantics from prototype activations. We extract the prototype activation vector $s = \text{Enc}(x_0)$ and sample random noise $x_T \sim \mathcal{N}(0, \mathbf{I})$ to generate new images $\hat{x}(s, x_T)$. Fig. 2a presents one reconstructed image (using the same x_T) with three variations (using random x_T). The results show that the majority of semantic information in the images is accurately recreated, confirming that the prototypes effectively capture meaningful semantic features.

Interpolation. Given two images x_0^1 and x_0^2 , we first retrieve its corresponding prototype activation vector and starting noise by reverse DDIM process: (s^1, x_T^1) and (s^2, x_T^2) , and then generate new samples using $(\text{Lerp}(s^1, s^2; t), \text{Slerp}(x_T^1, x_T^2; t))$ for steps $t \in [0, 1]$, where Lerp/Slerp represents linear/spherical linear interpolation respectively. Results are shown in Fig. 2c.

Visualization of the learned prototypes and consistency validation. Unlike other autoencoder-based diffusion models, our approach is explicitly designed to yield an interpretable semantic latent space, where each prototype is trained to capture distinct semantic content. In practice, we realize this by amplifying a prototype’s activation and extracting the most responsive patch (see Sec. 3.3). Fig. 3a shows selected prototypes with their semantic visualizations, and Fig. 3b demonstrates that the most activated patches remain semantically consistent across samples.

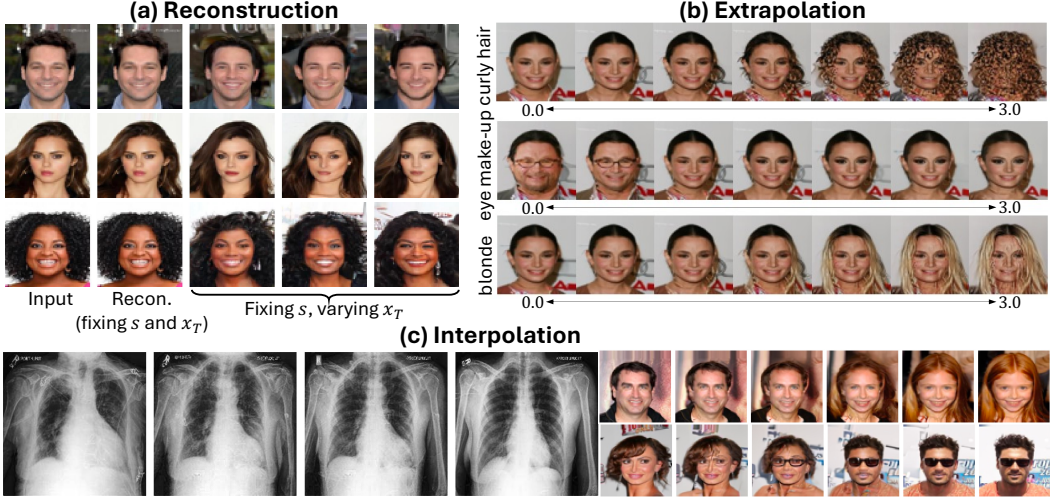


Figure 2: **Assessing the semantic meaning of the learned prototypes.** (a) Reconstruction. (b) Extrapolation. (c) Interpolation. Left: CheXpert, from 75-year-old female *w/o* enlarged heart (left) to 27-year-old male *w/* enlarged heart (right). Right: 2 examples from CelebA.

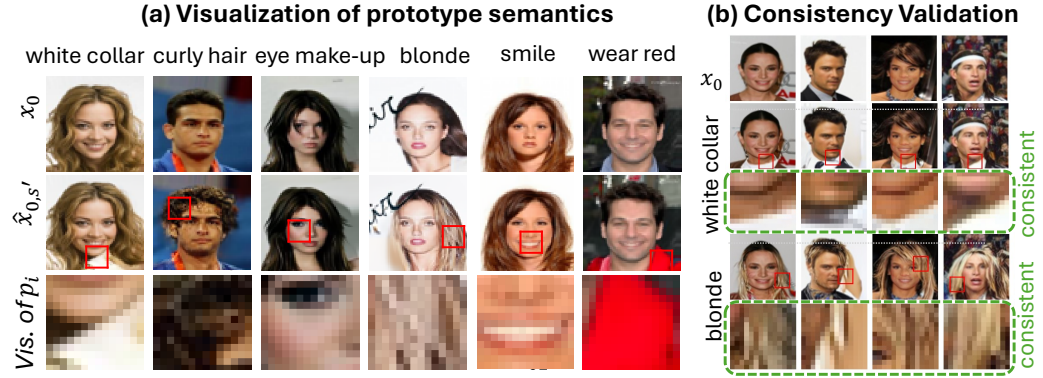


Figure 3: **Prototype visualization and consistency.** (a) Prototype visualization. Here, x_0 denotes the original image, $\hat{x}_{0,s'}$ denotes the generated image guided by condition s' , where s' is the enhanced prototype activation on j -th prototype. Red square highlights the most activated patch, which is considered as the visual representation of the chosen prototype, also shown in the third row. Note that prototype semantics are not pre-annotated but inferred through observation. (b) Visualization across random samples demonstrates that each prototype encodes consistent semantics.

Manipulation and extrapolation. By adjusting the condition s we can edit the image with specific semantic requests. Furthermore, pushing a selected dimension of s to extreme values (ranging from 0.0 to 3.0) results in a smooth and continuous enhancement of the associated semantic information, as demonstrated in Fig.2b. Unlike interpolation, which remains within the observed range, this process extends beyond the original data distribution, making it an *extrapolation*.

4.2 PROTOTYPE QUALITY

Prototype capability in semantic representation. We test the prototype quality via a downstream classification task on the prototype activation vectors s using a logistic regression classifier trained with 5-fold cross validation, reporting AUROC in Tab. 1 & 2. Our model outperform 3 out of 4 datasets in latent (prototype) quality, with particularly strong performance on CelebA and FFHQ. The lower latent quality for FMNIST may stem from *Patronus* prioritizing localized features, while DiffAE and InfoDiff emphasize global structures, which better capture the semantic information of

Table 1: **Prototype quality and generation quality on CelebA.**

	TAD \uparrow	Attrs \uparrow	Latent AUROC \uparrow	FID \downarrow
DiffAE	0.16 \pm 0.01	2.0 \pm 0.0	0.80 \pm 0.00	22.7 \pm 2.1
InfoDiff	0.30 \pm 0.01	3.0 \pm 0.0	0.84 \pm 0.00	23.6 \pm 1.3
<i>w/ learned z</i>	0.30 \pm 0.01	3.0 \pm 0.0	0.84 \pm 0.00	22.3 \pm 1.2
Patronus	0.43\pm0.02	9.0\pm0.0	0.87\pm0.00	14.6 \pm 0.1
<i>w/ learned s</i>	0.43\pm0.02	9.0\pm0.0	0.87\pm0.00	4.8\pm0.0

Table 2: **Prototype quality and generation quality on FashionMNIST, CIFAR-10, and FFHQ.**

	FMNIST		CIFAR-10		FFHQ	
	Latent AUROC \uparrow	FID \downarrow	Latent AUROC \uparrow	FID \downarrow	Latent AUROC \uparrow	FID \downarrow
DiffAE	0.84 \pm 0.00	8.2 \pm 0.3	0.40 \pm 0.01	32.1 \pm 1.1	0.61 \pm 0.00	31.6 \pm 1.2
InfoDiff	0.84\pm0.00	8.5 \pm 0.3	0.41 \pm 0.00	32.7 \pm 1.2	0.61 \pm 0.00	31.2 \pm 1.6
<i>w/ learned z</i>	0.84\pm0.00	7.4 \pm 0.2	0.41 \pm 0.00	31.5 \pm 1.8	0.61 \pm 0.00	30.9 \pm 2.5
Patronus	0.82 \pm 0.00	14.7 \pm 0.3	0.54\pm0.01	32.9 \pm 0.4	0.92\pm0.00	37.3 \pm 0.2
<i>w/ learned s</i>	0.82 \pm 0.00	2.6 \pm 0.1	0.54\pm0.01	8.0 \pm 0.1	0.92\pm0.00	24.1 \pm 0.1

FMNIST due to its high inter-class variability. For the datasets where semantic information is more localized, *Patronus* achieves a marked improvement.

Prototype disentanglement. We quantify the disentanglement on CelebA using TAD (Yeats et al., 2022). Following Wang et al. (2023b), we first remove the highly correlated attributes, then compute the AUROC score for each dimension of the prototype activation vector s . An attribute is “captured” if any dimension achieves AUROC > 0.75 . TAD is the sum of AUROC differences between the top two predictive dimensions per captured attribute. As shown in Tab. 1, *Patronus* outperforms previous models in both TAD and captured attributes.

4.3 GENERATION QUALITY

We assess generative quality using the Fréchet Inception Distance (FID), averaged over five random test sets of 10,000 images. Evaluation covers both unconditional and prototype-conditioned generation, where the latter incorporates learned prototype activation vectors from the test set (see Tab.1 & 2). *Patronus* significantly outperforms previous methods in prototype-conditioned generation across all four datasets. In the unconditional setting, it achieves state-of-the-art performance on CelebA and remains competitive on others; noting that its effectiveness depends on the training quality of both *Patronus* and the latent diffusion model.

4.4 DIAGNOSING SHORTCUT LEARNING IN DIFFUSION MODELS

We manipulated a subset of CelebA to introduce an unwanted correlation between hair color and smile: all blonde/brown-haired images smile, while black-haired ones do not. Results confirm the model captures the introduced bias, as increasing the black hair prototype shifts the smile property from “smile” to “non-smile” and vice versa (see Fig. 4a). Similar patterns emerge without subset manipulation. In Fig. 2b, decreasing “eye makeup” reduces female features. This emphasizes how *Patronus* can be utilized to discover unwanted model behavior, such as shortcut learning in this case.

5 DISCUSSION AND CONCLUSION

Prototypes Emerge at Different Times during Generation. Given a generated image, *Patronus* reveals *when* each prototype emerges in the generation process by obtaining the prototype similarity score from estimated \hat{x}_0 at each timestep (more details in Appendix), as shown in the top-right corner of Fig. 1a. Thus, by subtracting the two time-sequential s of the semantically-enhanced image $\hat{x}_{0,s'}$ and x_0 , we illustrate how each prototype emerges temporally in the diffusion process. As shown in Fig. 4b, none of the prototypes have a significant emergence in the first 200 stages of generation. Interestingly, prototypes relating to lower spatial frequency attributes appear earlier

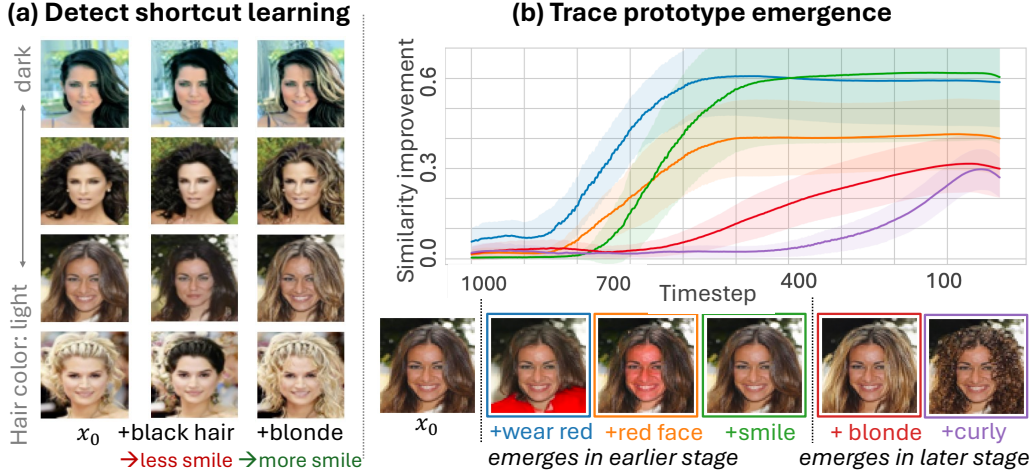


Figure 4: **Patronus as an interpretable tool** for (a) **Detecting shortcut learning**. Enhancing hair-color prototypes reveals their correlation with other attributes (e.g., smile), thereby exposing unwanted biases. (b) **Tracing prototype emergence**. Different prototypes appear at different stages of the diffusion process, as indicated by similarity score improvements, which provides insights for more effective image editing strategies.

during generation, such as “wearing red”; while higher spatial frequency attributes, like “curly hair”, emerge later in the generation process. This insight could potentially improve the efficiency of image editing or counterfactual generation by guiding how far an image should be reversed in the diffusion process. It could also support bias mitigation by leveraging the same mechanism once unwanted correlations are detected.

Prototype Correlation and Collapse. We test whether correlation between prototypes is caused by *prototype collapse*, where multiple prototypes represent the same semantics. To assess this, we introduce a Prototype Distinct Loss to encourage prototype disentanglement and evaluate its impact compared to using the denoiser loss alone. The Prototype Distinct Loss is defined as: $\mathcal{L}_{distinct} = \frac{1}{N} \sum_{i=1}^N \max(0, \delta - \min_{j \neq i} D_{ij})$, where D is the cosine distance with absolute similarity: $D_{ij} = 1 - \left| \frac{\mathbf{p}_i \cdot \mathbf{p}_j}{\|\mathbf{p}_i\| \|\mathbf{p}_j\|} \right|$. The margin δ is set to 0.5 and 1.0, where $\delta = 1.0$ enforces prototypes to be orthogonal. We initialize the new model using the original network parameters and train it for an additional 100 epochs using $\mathcal{L}_{ddpm} + \mathcal{L}_{distinct}$. Results show that the new models do not see a substantial change in the learned prototypes, suggesting that the prototypes optimized via the denoising objective are already sufficiently decorrelated without explicit regularization (see Appendix).

Do We Capture All Relevant Attributes? While *Patronus* shows great ability in capturing attributes, we notice that global features, e.g. gender and age, are harder to find in one specific prototype. This could result from the patch-based prototypical encoder, making non-local features hard to capture. See Appendix for illustrative visual examples.

5.1 CONCLUSION

We propose *Patronus*, an interpretable diffusion model integrated with a prototypical network. It enables intuitive interpretation of the generation process by visualizing learned prototypes (*what*) and identifying *where* and *when* they appear. It also supports semantic manipulation through prototype activation vector. Experiments show that *Patronus* achieves competitive performance and learns meaningful prototype-based representations. We further explore its capability to diagnose unwanted correlations in the generative process. We believe *Patronus* offers valuable insights into interpretable diffusion models by bridging diffusion and prototypical networks.

ACKNOWLEDGEMENTS.

Work on this project was partially funded by DTU Compute, the Technical University of Denmark; the Pioneer Centre for AI (DNRF grant nr P1); and the Novo Nordisk Foundation through the Center for Basic Machine Learning Research in Life Science (MLLS, grant NNF20OC0062606). The funding agencies had no influence on the writing of the manuscript nor on the decision to submit it for publication.

REFERENCES

Chaofan Chen, Oscar Li, Daniel Tao, Alina Barnett, Cynthia Rudin, and Jonathan K Su. This looks like that: deep learning for interpretable image recognition. *Advances in neural information processing systems*, 32, 2019.

Jon Donnelly, Alina Jade Barnett, and Chaofan Chen. Deformable protopnet: An interpretable image classifier using deformable prototypes. In *Proceedings of the IEEE/CVF conference on computer vision and pattern recognition*, pp. 10265–10275, 2022.

Gaurav R Ghosal and Reza Abbasi-Asl. Multi-modal prototype learning for interpretable multivariate time series classification. *arXiv preprint arXiv:2106.09636*, 2021.

Ian Goodfellow, Jean Pouget-Abadie, Mehdi Mirza, Bing Xu, David Warde-Farley, Sherjil Ozair, Aaron Courville, and Yoshua Bengio. Generative adversarial nets. *Advances in neural information processing systems*, 27, 2014.

René Haas, Inbar Huberman-Spiegelglas, Rotem Mulayoff, Stella Graßhof, Sami S Brandt, and Tomer Michaeli. Discovering interpretable directions in the semantic latent space of diffusion models. In *2024 IEEE 18th International Conference on Automatic Face and Gesture Recognition (FG)*, pp. 1–9. IEEE, 2024.

Jonathan Ho, Ajay Jain, and Pieter Abbeel. Denoising diffusion probabilistic models. *Advances in neural information processing systems*, 33:6840–6851, 2020.

Jeremy Irvin, Pranav Rajpurkar, Michael Ko, Yifan Yu, Silviana Ciurea-Ilcus, Chris Chute, Henrik Marklund, Behzad Haghgoo, Robyn Ball, Katie Shpanskaya, et al. Chexpert: A large chest radiograph dataset with uncertainty labels and expert comparison. In *Proceedings of the AAAI conference on artificial intelligence*, volume 33, pp. 590–597, 2019.

Tero Karras. A style-based generator architecture for generative adversarial networks. *arXiv preprint arXiv:1812.04948*, 2019.

Diederik P Kingma and Max Welling. Auto-encoding variational bayes. *arXiv preprint arXiv:1312.6114*, 2013.

Alex Krizhevsky, Geoffrey Hinton, et al. Learning multiple layers of features from tiny images. 2009.

Mingi Kwon, Jaeseok Jeong, and Youngjung Uh. Diffusion models already have a semantic latent space. *arXiv preprint arXiv:2210.10960*, 2022.

Sangyun Lee, Gayoung Lee, Hyunsu Kim, Junho Kim, and Youngjung Uh. Diffusion models with grouped latents for interpretable latent space. In *ICML 2023 Workshop on Structured Probabilistic Inference & Generative Modeling*, 2023.

Yipeng Leng, Qiangjuan Huang, Zhiyuan Wang, Yangyang Liu, and Haoyu Zhang. Diffusegæ: controllable and high-fidelity image manipulation from disentangled representation. In *Proceedings of the 5th ACM International Conference on Multimedia in Asia*, pp. 1–7, 2023.

Oscar Li, Hao Liu, Chaofan Chen, and Cynthia Rudin. Deep learning for case-based reasoning through prototypes: A neural network that explains its predictions. In *Proceedings of the AAAI Conference on Artificial Intelligence*, volume 32, 2018.

Ziwei Liu, Ping Luo, Xiaogang Wang, and Xiaoou Tang. Deep learning face attributes in the wild. In *Proceedings of International Conference on Computer Vision (ICCV)*, December 2015.

Sasha Luccioni, Christopher Akiki, Margaret Mitchell, and Yacine Jernite. Stable bias: Evaluating societal representations in diffusion models. *Advances in Neural Information Processing Systems*, 36:56338–56351, 2023.

Yao Ming, Panpan Xu, Huamin Qu, and Liu Ren. Interpretable and steerable sequence learning via prototypes. In *Proceedings of the 25th ACM SIGKDD International Conference on Knowledge Discovery & Data Mining*, pp. 903–913, 2019.

Yong-Hyun Park, Mingi Kwon, Jaewoong Choi, Junghyo Jo, and Youngjung Uh. Understanding the latent space of diffusion models through the lens of riemannian geometry. *Advances in Neural Information Processing Systems*, 36:24129–24142, 2023.

Konpat Preechakul, Nattanat Chatthee, Suttisak Wizadwongsa, and Supasorn Suwajanakorn. Diffusion autoencoders: Toward a meaningful and decodable representation. In *Proceedings of the IEEE/CVF conference on computer vision and pattern recognition*, pp. 10619–10629, 2022.

Yiting Qu, Xinyue Shen, Xinlei He, Michael Backes, Savvas Zannettou, and Yang Zhang. Unsafe diffusion: On the generation of unsafe images and hateful memes from text-to-image models. In *Proceedings of the 2023 ACM SIGSAC conference on computer and communications security*, pp. 3403–3417, 2023.

Chenyang Si, Ziqi Huang, Yuming Jiang, and Ziwei Liu. Freeu: Free lunch in diffusion u-net. In *Proceedings of the IEEE/CVF Conference on Computer Vision and Pattern Recognition*, pp. 4733–4743, 2024.

Narek Tumanyan, Michal Geyer, Shai Bagon, and Tali Dekel. Plug-and-play diffusion features for text-driven image-to-image translation. In *Proceedings of the IEEE/CVF Conference on Computer Vision and Pattern Recognition*, pp. 1921–1930, 2023.

Nikhil Vyas, Sham M Kakade, and Boaz Barak. On provable copyright protection for generative models. In *International conference on machine learning*, pp. 35277–35299. PMLR, 2023.

Chong Wang, Yuyuan Liu, Yuanhong Chen, Fengbei Liu, Yu Tian, Davis McCarthy, Helen Frazer, and Gustavo Carneiro. Learning support and trivial prototypes for interpretable image classification. In *Proceedings of the IEEE/CVF International Conference on Computer Vision*, pp. 2062–2072, 2023a.

Yingheng Wang, Yair Schiff, Aaron Gokaslan, Weishen Pan, Fei Wang, Christopher De Sa, and Volodymyr Kuleshov. Infodiffusion: Representation learning using information maximizing diffusion models. In *International Conference on Machine Learning*, pp. 36336–36354. PMLR, 2023b.

Han Xiao, Kashif Rasul, and Roland Vollgraf. Fashion-mnist: a novel image dataset for benchmarking machine learning algorithms. *arXiv preprint arXiv:1708.07747*, 2017.

Eric Yeats, Frank Liu, David Womble, and Hai Li. Nashae: Disentangling representations through adversarial covariance minimization. In *European Conference on Computer Vision*, pp. 36–51. Springer, 2022.